Advances in Radiation Oncology (2025) **10**, 101883

advances in radiation oncology

www.advancesradonc.org

Scientific Article

Functional Dose-Volume Analysis Based on a Novel Image Biomarker Derived From Dynamic Contrast-Enhanced Magnetic Resonance Imaging for Predicting Poststereotactic Body Radiation Therapy Liver Function Preservation in Patients With Hepatocellular Carcinoma

Yimin Ni, MSc,[a] Ho-Fun Victor Lee, MD,[b] Chi-leung Chiang, MD,[b] Lai-Yin Andy Cheung, PhD,[c] Zhengxing Huang, PhD,[d] Xinzhi Teng, PhD,[a] Jiang Zhang, PhD,[a] Ge Ren, PhD,[a] Jing Cai, PhD,[a,*] and Tian Li, PhD[a,*]

[a]Department of Health Technology and Informatics, The Hong Kong Polytechnic University, Hong Kong SAR, China; [b]Department of Clinical Oncology, The University of Hong Kong, Hong Kong SAR, China; [c]Department of Clinical Oncology, St. Paul's Hospital, Hong Kong SAR, China; and [d]Department of Biomedical Engineering, Zhejiang University, Zhejiang, China

Received 25 April 2025; accepted 12 August 2025

Purpose: The purpose of this study is to identify functional dose-volume parameters based on image biomarker derived from dynamic contrast-enhanced magnetic resonance imaging (DCE-MRI) for predicting poststereotactic body radiation therapy (SBRT) liver function deterioration (LFD) in patients with hepatocellular carcinoma.

Methods and Materials: Forty-eight patients treated with SBRT were retrospectively included. All patients underwent gadoxetate-enhanced DCE-MRI before treatment. Equivalent uniform dose, absolute dose-volume parameters including Dxcc and VxGy(cc) were calculated in 3 liver volumes: the anatomic volume (AV), the high-functional volumes (HFV) defined based on DCE-MRI derived function map, and the low-functional volume (LFV = AV − HFV). The primary endpoint of this study was the LFD as indicated by Δalbumin-bilirubin $\geq$ 0.5 at 1-month post-SBRT. Dose-volume parameters in patients with and without LFD were compared. Univariate logistic regression models were built to assess the ability of dose-volume parameters to distinguish between LFD and non-LFD cases.

Results: Of the 48 patients, 12 (25%) had LFD (Δalbumin-bilirubin $\geq$ 0.5). The dose-volume parameters in the AV and LFV were not statistically different in patients with and without LFD ($P > .005$), while D300cc, D400cc, and V10Gy(cc) of the HFV were significantly higher in patients with LFD than in the non-LFD group ($P < .005$). For distinguishing LFD and non-LFD cases, the mean area under curves (AUCs) for D300cc of AV, LFV, and HFV are 0.60, 0.50, and 0.78, respectively. The mean AUCs for D400cc of AV, LFV, and HFV are 0.62, 0.50, and 0.78, respectively. The mean AUCs for V10Gy of AV, LFV, and HFV are 0.63, 0.48, and 0.77, respectively.

Sources of support: This research was supported by the National Natural Science Foundation of China Young Scientist Fund (NSFC-YSF 82202941), the Innovation and Technology Support Programme (ITS/049/22FP), the research grants of General Research Fund (GRF 15104822, GRF 15102219), Health and Medical Research Fund (HMRF 10211606, HMRF 06173276), and the Research Project Grant of the National Institutes of Health (NIH R01 CA226899).

Research data are not available at this time.

*Corresponding authors: Tian Li, PhD; Email: litian.li@polyu.edu.hk and Jing Cai, PhD; Email: jing.cai@polyu.edu.hk

https://doi.org/10.1016/j.adro.2025.101883

Conclusions: The dose-volume parameters derived from HFV were linked to the risk of post-SBRT LFD. These functional parameters derived based on DCE-MRI could be useful to guide more personalized SBRT planning to protect liver function.

Introduction

Hepatocellular carcinoma (HCC) is the most prevalent form of primary liver cancer and ranks fourth in cancer-related mortality worldwide.[1] The global 5-year survival rate for patients with HCC is estimated to be between 5% and 30%.[2,3] While hepatectomy and liver transplantation are the standard treatments, over 70% of patients with HCC have liver dysfunction, making them unsuitable for surgical interventions.[4,5] Stereotactic body radiation therapy (SBRT) has emerged as an alternative, offering 1-year local control rates of 65% to 100% for HCC[6] and 90% to 100% for oligometastases.[7] However, SBRT can be associated with significant toxicity in certain settings, particularly if critical factors such as baseline liver function and proximity to organs at risk are not rigorously considered. Reported toxicities include grade ≥3 events in up to 38% of patients,[6] deaths from liver failure in up to 13%, and high-grade luminal toxicities in up to 11% of patients.[8] These risks underscore the importance of careful patient, target, and dose selection.

Current radiation therapy planning relies on anatomic dose-volume constraints to mitigate radiation-induced liver toxicity (RILT), where a uniform hepatic function is simplistically assumed.[9-11] However, in patients with HCC, the regional distribution of hepatic function can be heterogeneous due to underlying liver diseases such as inflammation, fibrosis, and cirrhosis. Under the current SBRT planning protocol, RILT is observed in 10% to 30% of patients with HCC within 1 to 3 months posttreatment.[12] To reduce the risk of RILT, functional liver-image guided hepatic therapy has been proposed. Examples of functional liver-image guided hepatic therapy include the use of single-photon emission computed tomography,[13,14] positron emission tomography,[15] dual-energy computed tomography (DECT),[16] and contrast-enhanced magnetic resonance imaging (MRI)[17] for the delineation of functional volume and function avoidance planning, aiming for a better-preserved functional liver volume without compromising the planning target volume (PTV) coverage and organ-at-risk (OAR) sparing. However, the definition of functional liver tissue is variable across different studies, and no consensus has been reached regarding the dose constraints for delineated functional volumes. In addition, no correlation has been established between the dose-volume parameters of functional volume and posttreatment outcomes.

Dynamic contrast-enhanced magnetic resonance imaging (DCE-MRI) is routinely used in clinics for qualitative and quantitative evaluation of the HCC and liver parenchyma regions.[18] Previous studies have primarily focused on deconvolution analysis and pharmacokinetic tissue-compartment modeling to assess the tumor microenvironment.[19,20] More recent research has demonstrated a statistically significant correlation between the accumulation of signal intensity on gadoxetate DCE-MRI and fibrosis staging as well as liver function status.[21,22] And a successful correlation between gadoxetate DCE-MRI and post-SBRT liver functional changes has been established,[23] suggesting DCE-MRI's potential in guiding function avoidance planning for SBRT.

Given its quantitative and accessible nature, identifying DCE-MRI-derived image biomarkers for function preservation following SBRT could potentially lead to improved treatment outcome. However, there is currently a lack of data that establishes a correlation between the incidence of RILT and SBRT dose-volume parameters specific to patients with HCC. In this retrospective study, we attempted to bridge this gap by examining the association between post-SBRT liver function deterioration (LFD) and dose-volume parameters derived from functional mapping on DCE-MRI.

Methods and Materials

Study design and patient data

This is a single-center study aimed to identify dose-volume parameters based on DCE-MRI functional mapping for post-SBRT liver function preservation. This study was ethically and scientifically reviewed and approved by the institutional review board committee. A total of 48 patients who were treated with SBRT between July 2016 and June 2020 were retrospectively analyzed. All patient data have been anonymized with identical information eradicated before reception. The inclusion criteria included: (1) age between 18 and 80 years old; (2) pathologically confirmed unresectable HCC based on the American Association for the Study of Liver Diseases practice guideline 2010; (3) lesion diameter between 5 and 15 cm; (4) number of lesions ≤3; (5) Child−Pugh score A5-B7; (6) liver minus gross-target-volume >700 cc.

Radiation therapy details

All patients received a total dose of 30 Gy to 50 Gy in 5 fractions, based on the OAR constraints with intervals of

24 to 72 hours between fractions. The total treatment course was completed within 5 to 10 days. The average and maximum intensity projection volumes were reconstructed via the sorted 4-dimensional CT phases. The internal target volume (ITV) was delineated on maximum intensity projection series to account for tumor motion. The PTV was determined by expanding the ITV in superior and inferior direction. The liver OAR was defined as the volume of liver parenchyma minus the ITV. Varian External Beam Planning Software, Eclipse (Varian Medical Systems) was used for treatment planning. Dose constraints to abdominal OARs followed the international guidelines.[24] Liver SBRT was performed on Varian TrueBeam linear accelerator using 6 MV or 10 MV photon beams with the respiratory motion monitored by the real-time position management gating system. Cone beam CT image guidance was used to confirm the tumor position before each treatment.

DCE-MRI acquisition

The pretreatment DCE-MRI was acquired with gadoxetic acid as the contrast agent using 1.5 Tesla Signa system (GE Healthcare) or 3 Tesla Achieva system (Philips Healthcare) with a 12- or 16-channel phased-array body coil. The acquisition followed the sequential trans-arterial chemoembolization and stereotactic body radiotherapy followed by immunotherapy and liver imaging reporting and data system ver.2017 protocols with the following parameters: slice thickness = 3 mm, field-of-view = 360 to 400 mm^2, slice number = 140 to 152 slices, and voxel size = 0.625 × 0.625 × 3 mm^3, all in the transverse plane. The time window between DCE-MRI acquisition and simulation CT was 24 to 48 hours. The acquisition of DCE-MRI starts at the pre-contrast phase as a baseline followed by gadoxetic acid disodium (Gd-EOB-DTPA) injection into the cubital vein with a dose of 0.1 mL/kg using a power injector. The infusion flow rate was set to 1 mL/s, which was followed by normal saline at the same flow rate. Subsequently, the arterial phase was acquired, followed by the portal-venous phase, 3-minute delayed phase, 10-minute delayed phase, and the hepatobiliary phase at 15 to 20 minutes after injection. Each of the three-dimensional image volumes was acquired within a single breath-hold.

Image postprocessing and analysis

DCE-MRI volumes of different phases were coregistered to the corresponding planning CT using a deformable image registration method with the Elastix toolbox.[25] The registration accuracy was visually inspected to ensure the distance difference between CT and DCE-MRI for the liver and gross-target-volumes did not exceed the TG132 recommendation of 3 mm.[26] The ITV and OAR contours were manually delineated by a clinical oncologist (with >15 years of experience) on the axial planning CT. SBRT dose distributions were resampled to match the same size of planning CT for further processing. The delineated liver parenchyma minus PTV region was selected as the region of interest.

For each patient, the liver signal intensities were normalized by the average signal intensity of a selected spleen subregion to obtain the normalized signal intensity (nSI) for each voxel. Quantitative indices derived from the deformed DCE-MRI included the relative liver enhancement (RLE), the initial area under curve (iAUC), and the maximum enhancement (E_{max}). RLE is defined as the relative nSI increasement of time t comparing to the nSI before contrast injection: $RLE_t = (nSI_t - nSI_{pre})/nSI_{pre}$. iAUC is calculated as the accumulated nSI from time t_0 to a given time t: $iAUC_t = \int_{t_0}^{t} nSI(t)dt$. E_{max} is the maximum enhancement across all phases: $E_{max} = max(\mathrm{n}SI(t))$. The Pearson correlation analysis was used to examine the relationship between these DCE-MRI-derived indices and the liver function as indicated by albumin-bilirubin (ALBI) scores. The iAUC-20 min was selectively used to determine a threshold value for distinguishing high-functional liver volumes from low-functional volumes (LFVs).

Clinical endpoint

The clinical endpoint of the study was acute LFD at 1 month post-SBRT, defined as an increase in the ALBI score of ≥0.5 from baseline. The threshold of ΔALBI ≥ 0.5 was selected based on a prior clinical validation study which demonstrates this magnitude of change has significant prognostic value for hepatic toxicity.[27] This was evaluated retrospectively using biochemical tests conducted 1 month after SBRT. The 1-month post-SBRT timepoint was chosen to capture early biochemical changes during the window of acute radiation hepatopathy onset and peak transaminitis, leverage the validated prognostic value of early ALBI score changes, and minimize confounding by later events like tumor progression or systemic therapies. Patients were initially categorized into 3 groups based on their baseline ALBI score: grade I (≤ −2.60), grade II (−2.60 to −1.39), and grade III (>−1.39), indicating worsening liver impairment. They were further classified by liver function changes: improved (ΔALBI ≤ −0.5), stable (−0.5 < ΔALBI < 0.5), and deteriorated liver function (ΔALBI ≥ 0.5) for subsequent analysis.

Statistical analysis

The dose-volume parameters used to predict post-SBRT LFD includes: (1) equivalent uniform dose, (2) dose received by x cc of the total volume (Dxcc, x = 100-800), and (3) volumes (in cc) receiving xGy of dose (VxGy,

x = 5-30). These dose-volume parameters were calculated in 3 liver volumes: the conventional anatomic volume (AV), the high-functional liver volumes defined on DCE-MRI derived function map (HFV), and the LFV (LFV = AV-HFV). The primary endpoint of this study was the LFD as indicated by ΔALBI ≥0.5 worsening at 1-month posttreatment. For each of the dose-volume parameters studied, a Wilcoxon test was employed to assess the statistical difference between treatment response (ie, LFD or non-LFD) of these parameters. The Bonferroni correction was applied to all the analyses to account for the increase of familywise error rate caused by multiple analyses.[28] Parameters with P values of <.005 were considered statistically significant. Univariate logistic regression models were built with the area under the receiver operating curves (AUC) calculated to assess the predictive abilities of dose-volume parameters in distinguishing between LFD and non-LFD cases. As a result of the small sample size, multivariate statistical testing was not conducted. All statistical analysis was performed using MATLAB R2021b.

Results

Patient characteristics

Between July 2016 and June 2020, 48 patients with primary (n = 24), recurrent (n = 22), and metastatic (n = 2) HCC were included in this retrospective study. The demographics, clinical, and SBRT prescription details are outlined in Table 1. Of these, 12 patients were grouped as LFD (11 male; median age 69 [IQR, 60-76]) and 36 as non-LFD (23 male; median age 68 [IQR, 64-74]). Cirrhosis was confirmed in 34 patients. Twenty-one out of the 22 recurrent patients had received prior liver-directed therapies, including transarterial chemoembolization, high-intensity focused ultrasound, radiofrequency ablation, wedge resection, sectionectomy, and hepatectomy. The nontumor-bearing liver absolute volume and the corresponding functional subvolumes (HFV and LFV) showed no statistically significant difference between LFD and non-LFD groups. The baseline ALBI grades of the patients were 21 grade I, 25 grade II, and 2 grade III. The median international normalized ratio of the patients was 1.2 (IQR, 1.1-1.3). Median platelet counts were 58 (IQR, 51-113) for LFD and 128 (IQR, 95-162) for non-LFD patients. Four, 8, 6, 13, and 17 patients received 5 fractions of 6 Gy each, 7.5 Gy each, 8 Gy each, 9 Gy each, and 10 Gy each, respectively.

Quantitative DCE-MRI indices as indicators of liver function

Three quantitative indices were derived from multiphase DCE-MRI: RLE (relative signal increase), iAUC (signal accumulation), and E_{max} (maximum enhancement). Figure 1 shows the Pearson correlation between these indices and liver function (ALBI scores). Low correlations were observed for RLE-3 min, RLE-10 min, and RLE-20 min. Moderate correlations appeared in iAUC-3 min and iAUC-10 min, while high correlations were found in iAUC-20 min and E_{max}. Among these, iAUC-20 min had the highest correlation with ALBI scores, followed by E_{max}.

Figure 2 illustrates the distribution of 3 selected DCE-MRI indices across different ALBI grades. For RLE-20 min, no significant difference was found between ALBI grade I and grades II/III (1.45 vs 1.09, P = 0.134). However, E_{max} and iAUC-20 min were significantly higher in ALBI grade I compared to grades II/III: E_{max} (3.19 vs 2.55, P = 2.01e−4) and iAUC-20 min (49.34 vs 41.73, P = 2.17e-4). Based on these results, iAUC-20 min, which showed the highest correlation with liver function, was used to determine a threshold for distinguishing high-functional from low-functional liver volumes. A threshold value of 46 was established, stratifying the 75th percentile of ALBI grade II/III (45.74) and the 25th percentile of ALBI grade I (46.58) in the iAUC-20 min distributions (Fig. 2C).

Functional dose-volume parameters as predictors for post-SBRT liver function change

Using the iAUC-20 min threshold, liver parenchyma is divided into subregions based on functionality: HFV (iAUC-20 min ≥ 46), LFV (iAUC-20 min < 46), and the conventional AV (AV = HFV + LFV). Dose distribution comparisons between patients with LFD and those without are shown in Fig. 3A. DVH distributions for LFV and AV were similar across groups, but differences were observed in HFV.

Figure 3B presents boxplots of functional dose-volume parameters for patients with improved (ΔALBI < −0.5), stable (−0.5 ≤ ΔALBI < 0.5), or deteriorated (ΔALBI ≥ 0.5) liver function post-SBRT. Supporting documents include additional parameters like mean liver dose (MLD), Dx% (dose received by x% of total volume), and VxGy (relative volumes receiving xGy of dose). Median D300cc, D400cc, and V10Gy in LFV and AV showed no statistical difference between groups. However, these indices were significantly higher in HFV for LFD patients: D300cc (10.98Gy vs 5.86Gy, P = .0044), D400cc (7.61Gy vs 2.23Gy, P = .0039), and V10Gy (327.45cc vs 194.83cc, P = .0050). The equivalent uniform dose of HFV was also higher in patients with LFD, though a P value of .04 suggests limited statistical significance.

Figure 4 displays receiver operating curves assessing the ability of functional dose-volume parameters to distinguish patients with LFD. Parameters include D300cc, D400cc, and V10Gy(cc) for HFV, LFV, and AV. AUCs

Table 1 Patient, tumor, prior liver-directed therapy, baseline liver characteristics, and SBRT prescription of the analyzed cohort (48 patients)

Patient and tumor characteristics	Total* (n = 48)	Deteriorated* (n = 12)	Improved/stable* (n = 36)	*P* value†
Age (y)	68 (62-74)	69 (60-76)	68 (64-74)	.91
Male sex	34 (71%)	11 (92%)	23 (64%)	.07
Cirrhosis	34 (71%)	8 (67%)	26 (72%)	.73
Cancer type				.95
Primary	24 (50%)	6 (50%)	18 (50%)	
Recurrent	22 (46%)	6 (50%)	16 (44%)	
Metastasis	2 (4%)	0 (0%)	2 (6%)	
Prior liver-directed therapy (for recurrent patients only)‡				
TACE	14 (29%)	3 (25%)	11 (31%)	
HIFU	3 (6%)	1 (8%)	2 (6%)	
Radiofrequency ablation	6 (13%)	1 (8%)	5 (14%)	
Wedge resection	5 (10%)	0 (0%)	5 (14%)	
Hepatectomy/sectionectomy	4 (8%)	2 (17%)	2 (6%)	
Liver volume (cc)				
AV	1271 (1107-1441)	1302 (1232-1485)	1261 (1030-1422)	.41
HFV	779 (618-936)	817 (663-1031)	766 (602-932)	.51
LV	493 (333-631)	485 (327-643)	495 (341-630)	.51
Baseline liver biomarkers				
ALBI grade				.05
1 (≤−2.60)	21 (44%)	3 (25%)	18 (50%)	
2 (−2.60 to −1.39)	25 (52%)	9 (75%)	16 (44%)	
3 (>−1.39)	2 (4%)	0 (0%)	2 (6%)	
INR	1.2 (1.1-1.3)	1.25 (1.20-1.38)	1.1 (1.0-1.2)	<.01
Platelet count (per nanoliter blood)	119 (64-144)	58 (51-113)	128 (95-162)	<.01
SBRT dose				.06
30 Gy	4 (8%)	2 (17%)	2 (5%)	
37.5 Gy	8 (17%)	3 (25%)	5 (14%)	
40 Gy	6 (13%)	2 (17%)	4 (11%)	
45 Gy	13 (27%)	3 (25%)	10 (28%)	
50 Gy	17 (35%)	2 (17%)	15 (42%)	

Abbreviations: ALBI = albumin-bilirubin; AV = anatomic volume; HFV = high function volume; HIFU = high-intensity focused ultrasound; INR = international normalized ratio; LFD = liver function deterioration; LFV = low function volume; SBRT = stereotactic body radiation therapy; TACE = transarterial chemoembolization.

*The values listed are median (IQR) or number (%).

†*P* value < .05 indicates statistical significance between patients with/without LFD.

‡Some patients underwent multiple therapies.

for D300cc are 0.60 (AV), 0.50 (LFV), and 0.78 (HFV); for D400cc, 0.62 (AV), 0.50 (LFV), and 0.78 (HFV); for V10Gy(cc), 0.63 (AV), 0.48 (LFV), and 0.77 (HFV). For all 3 dose-volume parameters, the models built on HFV show better predictive ability than the ones derived from LFV and AV.

Figure 5 provides images of 2 patients with HCC treated with SBRT. Figure 5A shows a 68-year-old male (patient A) with improved liver function post-SBRT (ALBI score: −1.16 to −2.60), where HFV was spared from high-dose irradiation. Figure 5B shows a 50-year-old male (patient B) with deteriorated liver function

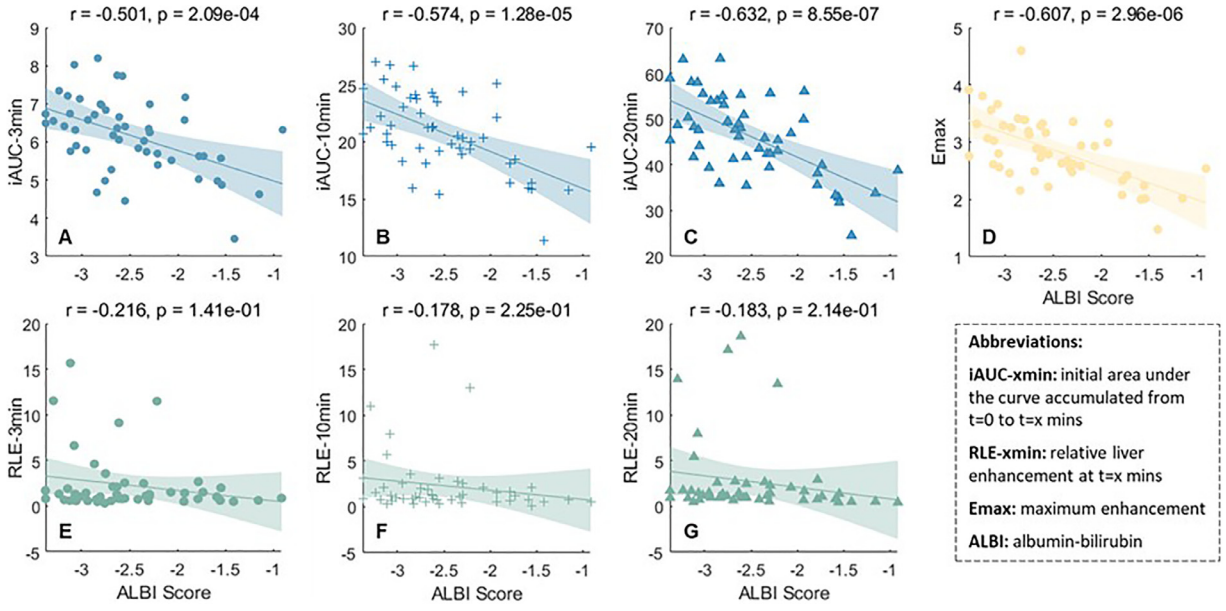

Figure 1 Scatterplots showing the correlation between dynamic contrast-enhanced magnetic resonance imaging (DCE-MRI)-derived indices and liver function representation (albumin-bilirubin [ALBI] scores). The DCE-MRI derived indices include: (A) initial area under curve (iAUC)-3 min ($r = -0.50$; $P < .001$), (B) iAUC-10 min ($r = -0.57$; $P < .001$), (C) iAUC-20 min ($r = -0.63$; $P < .001$), (D) E_{max} ($r = -0.61$; $P < .001$), (E) relative liver enhancement (RLE)-3 min ($r = -0.22$; $P = .14$), (F) RLE-10 min ($r = -0.18$; $P = .23$), and (G) RLE-20 min ($r = -0.18$; $P = .21$).

(ALBI score: −2.67 to −2.15), where HFV received higher doses compared to LFV.

Discussion

In this retrospective study, we explored the correlation between DCE-MRI-derived indices and liver function status, measured by the ALBI score. Figure 1 shows strong correlations between ALBI score and iAUC-20 min ($r = -0.63$; $P < .001$) and E_{max} ($r = -0.61$; $P < .001$), highlighting the potential of low-time-resolution DCE-MRI for liver function assessment. We also examined the link between post-SBRT liver function decline and dose-volume parameters from DCE-MRI functional mapping, finding that functional parameters are more effective than anatomic ones in predicting post-SBRT liver function decline. To our knowledge, this study is the first to correlate DCE-MRI functional mapped dose-volume parameters with acute post-SBRT liver function decline.

The ALBI score, an objective measure of liver function, is increasingly used for monitoring therapeutic outcomes in chronic liver disease patients. Unlike the subjective Child−Pugh score, the ALBI score is based on albumin and bilirubin levels. It correlates strongly with overall survival,[29,30] tumor relapse,[31] and liver failure[32,33] in patients undergoing curative treatments. It is also an independent predictor of survival, toxicity, and liver failure in radiation therapy patients.[34,35] Establishing a correlation between routine imaging modalities and the ALBI score bridges the gap between qualitative radiography and liver function assessment. DCE-MRI indices have proven useful for liver function monitoring.[21,22] Our study found higher correlations between ALBI score and iAUC-20 min and E_{max} compared to previous studies.[21]

Current HCC SBRT treatment planning relies on anatomic liver volumes without considering functional heterogeneity.[9-11] International guidelines recommend MLD not exceed 22 Gy and V10Gy be less than 68%.[24] A systematic review suggested a stricter MLD constraint of 15 Gy for SBRT plans.[12] However, patients who developed posttreatment LFD in our study had an MLD well below these thresholds (MLD = 11.56 Gy [IQR, 8.83-13.33 Gy]) and the observed mean V10Gy(%) (47.36% [IQR, 36.62%-52.98%]) is also below the recommended 68%. Thus, delivering hypofractionated high dose to the patients with HCC without considering functional preservation might lead to suboptimal treatment outcomes. In our analysis, the absolute nontumor-bearing liver volumes showed no significant difference between LFD and non-LFD groups (Table 1). While we recognize that absolute volumes provide important context, we maintain that the functional subvolumes (HFV/LFV) may offer more clinically actionable information for predicting radiation tolerance, as they account for interpatient variability in total liver size.

Consistent with standard clinical practice, all treatment plans in our study incorporated the constraint of sparing ≥700 cc of nontumor-bearing liver from receiving >15 Gy. Our dosimetric analysis confirms successful

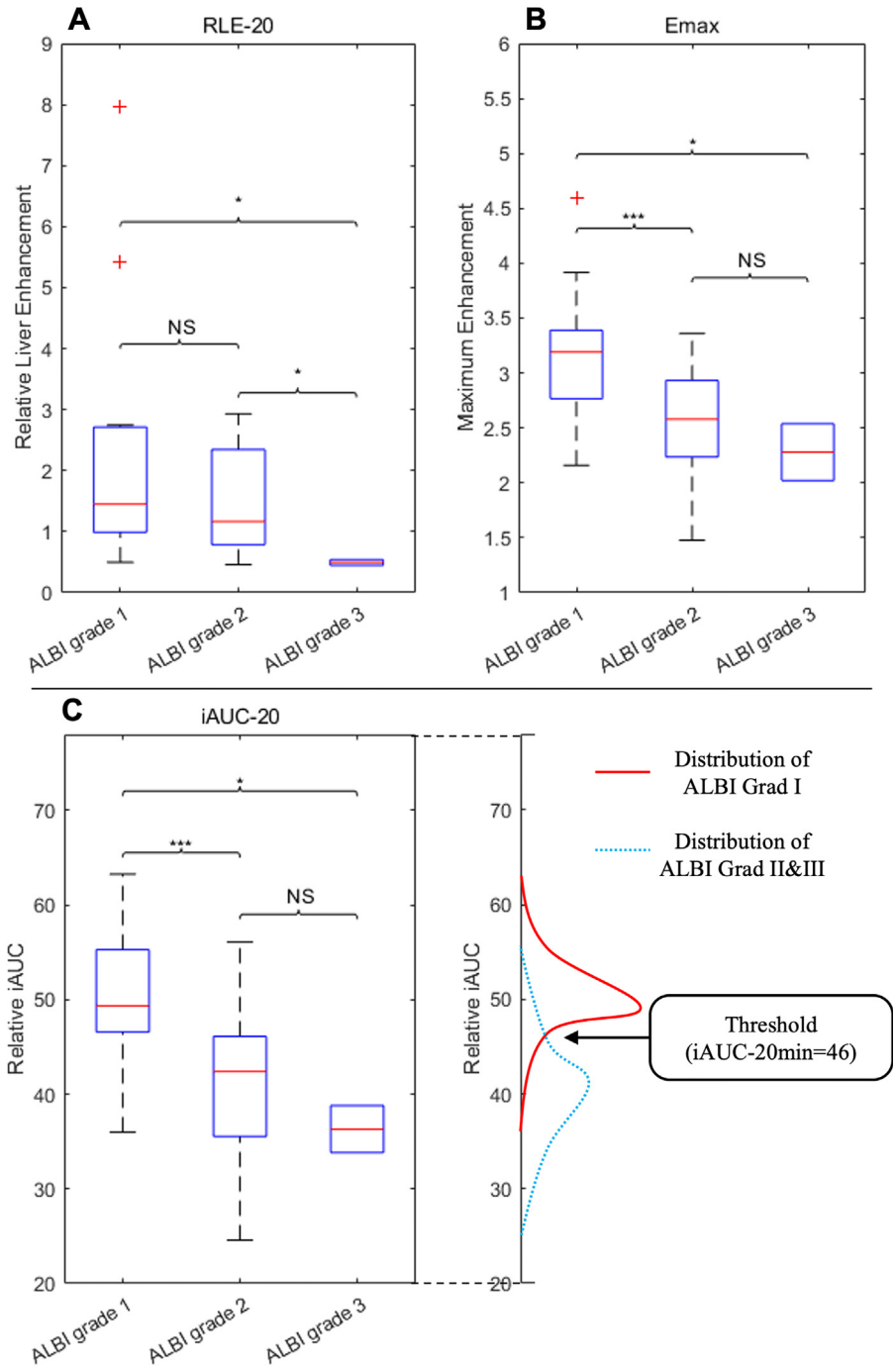

Figure 2 Box plots indicate the distribution of 3 selected dynamic contrast-enhanced magnetic resonance imaging (DCE-MRI) derived indices in patients with different albumin-bilirubin (ALBI) grades. The lower and upper borders of the plotted boxes are the 25th and 75th percentiles. The red lines within the boxes are the median values of each group. (A) relative liver enhancement (RLE)-20 mins, (B) E_{max}, (C) initial area under curve (iAUC)-20 mins. The threshold value was determined to stratify the 75-percentile of ALBI grade II/III (blue curve) and the 25-percentile of ALBI grade I (red curve) in the iAUC-20 mins distributions. * indicates $P <= .05$, *** indicates the difference is significant at alpha level corrected by the Bonferroni method. *Abbreviation:* NS = not statistically significant.

implementation of this constraint, with the mean dose to 700 cc of spared liver volume being 3.1 Gy for patients with LFD and 2.3 Gy for patients without LFD (Fig. 3A), both substantially below the threshold. Additional analysis further revealed that while V15Gy to LFV and AV showed no significant differences between groups, HFV V15Gy was significantly lower in patients without LFD compared to patients with LFD ($P < .05$; Fig. E6).

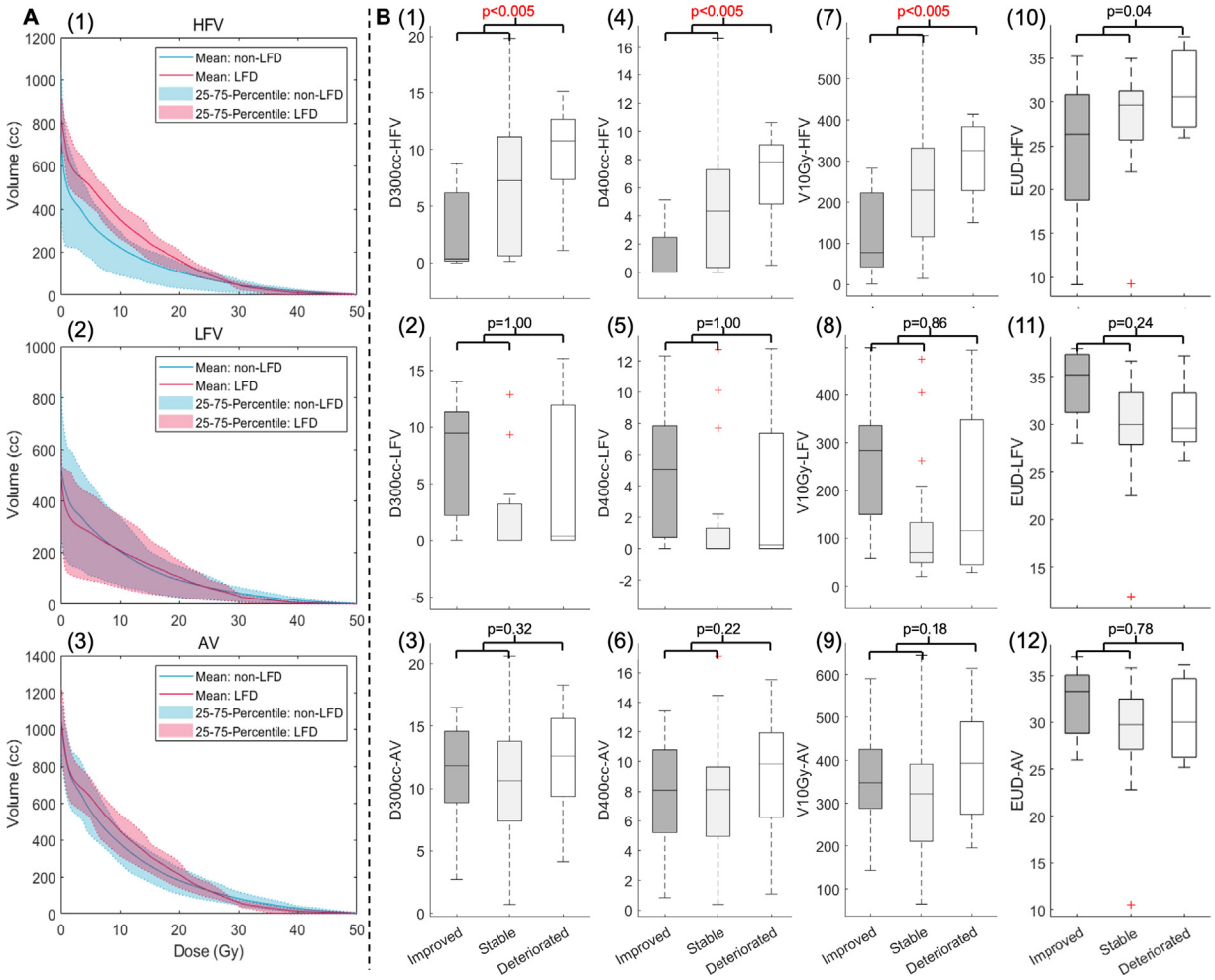

Figure 3 Dose-volume histogram (DVH) comparison between patients with and without liver function deterioration (LFD) calculated in absolute high function volume (HFV) (A.1), absolute low function volume (LFV) (A.2), absolute anatomic volume (AV) (A.3). And the corresponding boxplots indicating the distribution of dose-volume parameters in patients with improved, stable, or deteriorated liver functions post-stereotactic body radiation therapy (SBRT). The dose-volume parameters include: (B.1) D300cc of HFV, (B.2) D300cc of LFV, (B.3) D300cc of AV; (B.4) D400cc of HFV, (B.5) D400cc of LFV, (B.6) D400cc of AV; (B.7) V10Gy of HFV, (B.8) V10Gy of LFV, (B.9) V10Gy of AV; (B.10) equivalent uniform dose (EUD) of HFV, (B.11) EUD of LFV, (B.12) EUD of AV. The *P* values were calculated between LFD (deteriorated) and non-LFD (improved + stable) patient groups. The *P* values in red indicate the difference is significant at alpha level corrected by the Bonferroni method.

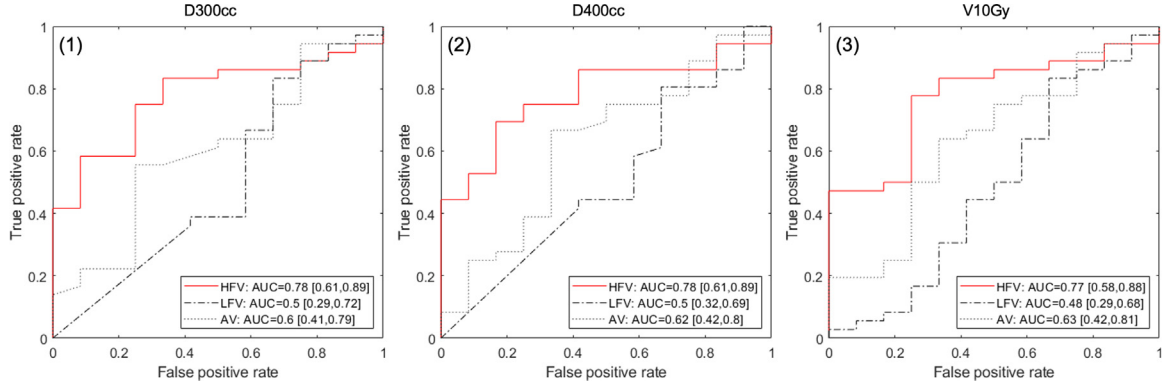

Figure 4 The receiver operating curves with mean area under curves (AUCs) and IQRs to assess the ability of (1) D300cc, (2) D400cc, and (3) V10Gy of high function volume (HFV), low function volume (LFV), and anatomic volume (AV) to distinguish between patients with and without liver function deterioration.

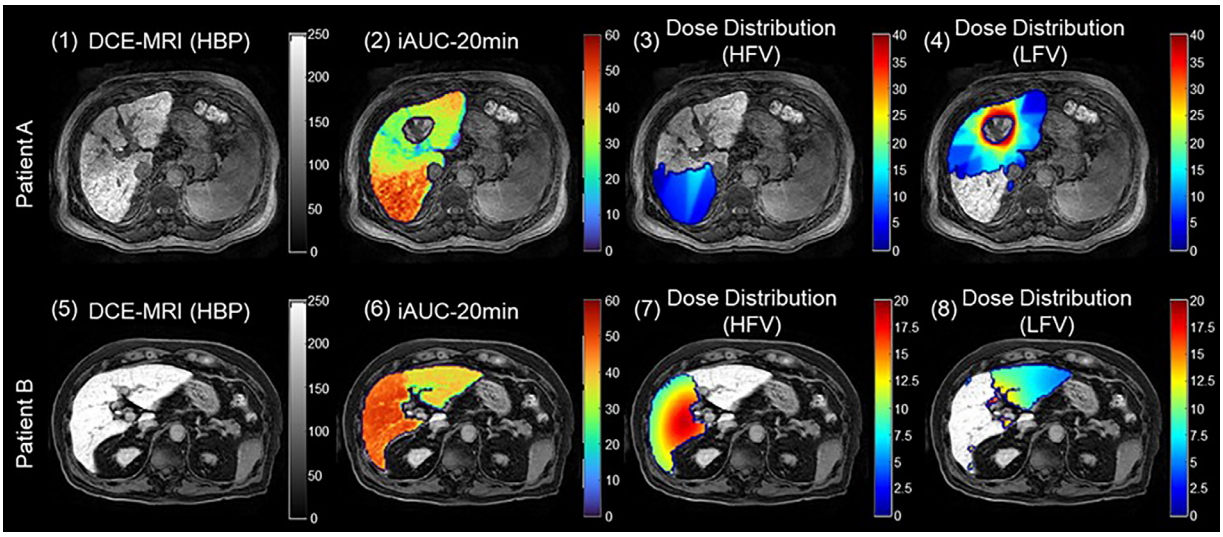

Figure 5 From left to right: contrast-enhanced magnetic resonance imaging (MRI) at hepatobiliary phase (HBP), color-coded initial area under curve (iAUC)-20 min maps, dose distribution in high function volume (HFV), and dose distribution in low function volume (LFV) in 2 participants with hepatocellular carcinoma (HCC) treated with stereotactic body radiation therapy (SBRT). Color scale indicated the magnitude of iAUC-20 min (unitless) or dose (Gy), with blue representing lower magnitudes and red representing higher magnitudes. (A) Patient A with improved liver function after SBRT. (B) Patient B with deteriorated liver function after SBRT. *Abbreviation*: DCE-MRI = dynamic contrast-enhanced magnetic resonance imaging.

This finding supports our hypothesis that radiation dose to HFV may be particularly relevant for predicting post-SBRT hepatotoxicity risk. While other studies reported a higher MLD in patients who developed RILT,[36,37] our study found no statistical significance for MLD of AV and HFV in predicting posttreatment LFD.

Efforts to reduce RILT from SBRT have led to safer treatment strategies. A liver function-based adaptive radiation therapy regime completed a phase II trial with 90 patients, showing a 95% local control rate of HCC with an 8% incidence of RILT.[38,39] This strategy features the adoption of radiation dose based on baseline and mid-treatment liver function measurement of 15-min indocyanine retention (ICGR15). Even though an improved liver toxicity was observed, this strategy considers only the global liver function without taking liver function heterogeneity into account. Other functional avoidance methods include using static contrast-enhanced MRI for liver functional area delineation. One publication in 2017 stated the feasibility of functional avoidance based on static contrast-enhanced MRI without compromising PTV coverage and the sparing of other OARs.[17] Nevertheless, no correlation has been established between dose-volume parameters of functional volume and posttreatment outcomes. The dosimetric analysis of our study may shed light on such correlations (as shown in Fig. 3B): unlike LFV and AV, the HFV-derived dose-volume parameters were significantly higher in patients with posttreatment LFD than the non-LFD group ($P < .005$).

Our study has several limitations. First, it was a single-institutional retrospective study with a small sample size (n = 48). The lack of standardized archives has hindered the spatial analysis of prior liver-directed therapies relative to functional liver subvolumes and potential confounding factors for LFD. While we established a correlation between post-SBRT LFD and dose-volume parameters from DCE-MRI functional mapping, larger multi-institutional studies are needed to generalize these findings. Second, liver parenchyma signal intensity normalization relied on manual region of interest selection of the spleen, which could introduce interobserver variability. We addressed this by visually inspecting each image volume and minimized MR and CT registration errors through manual quality checks. Additionally, RILT was defined by ALBI score changes without considering clinical factors like ascites, fatigue, and abdominal pain. Future studies should adopt a prospective design with closer monitoring of these factors. Lastly, although functional imaging techniques like single-photon emission computed tomography, positron emission tomography, and dual-energy computed tomography have been proposed for liver SBRT planning,[13-16] no correlation between their dose-volume parameters and treatment outcomes has been established. Comparing DCE-MRI with these modalities in future research could be valuable.

Conclusions

In this study, we identified an image biomarker based on DCE-MRE-derived index map (ie, iAUC-20 min) for differentiating high and lower liver function volumes. We assessed the correlation between dose-volume parameters derived from DCE-MRI functional mapping and post-

SBRT LFD. The functional parameters derived from DCE-MRI surpass standard anatomic dose-volume parameters in pinpointing the risk of post-SBRT LFD. They possess significant potential in guiding functional liver avoidance radiation therapy planning to better preserve the liver functions. To further implement this clinically, a more extensive study cohort and interventional trials are required.

Disclosures

The authors declare that they have no known competing financial interests or personal relationships that could have appeared to influence the work reported in this paper.

Acknowledgment

None

Declaration of AI and AI-Assisted Technologies in the Writing Process

During the preparation of this work the author(s) used ChatGPT-4 in order to improve language and readability. After using this tool/service, the author(s) reviewed and edited the content as needed and take(s) full responsibility for the content of the publication.

Supplementary materials

Supplementary material associated with this article can be found in the online version at doi:10.1016/j.adro.2025.101883.

References

1. Rumgay H, Ferlay J, Martel C, et al. Global, regional and national burden of primary liver cancer by subtype. *Eur J Cancer*. 2022;161:108-118.
2. Sarveazad A, Agah S, Babahajian A, Amini N, Bahardoust M. Predictors of 5 year survival rate in hepatocellular carcinoma patients. *J Res Med Sci*. 2019;24:86.
3. Hassanipour S, Vali M, Gaffari-Fam S, et al. The survival rate of hepatocellular carcinoma in Asian countries: A systematic review and meta-analysis. *EXCLI J*. 2020;19:108-130.
4. Pesapane F, Nezami N, Patella F, Geschwind JF. New concepts in embolotherapy of HCC. *Med Oncol*. 2017;34:58.
5. Bruix J, Sherman M. Practice guidelines committee. Management of hepatocellular carcinoma. *Hepatology*. 2005;42:1208-1236.
6. Murray LJ, Dawson LA. Advances in stereotactic body radiation therapy for hepatocellular carcinoma. *Semin Radiat Oncol*. 2017;27:247-255.
7. Wild AT, Yamada Y. Treatment options in oligometastatic disease: Stereotactic body radiation therapy - focus on colorectal cancer. *Visc Med*. 2017;33:54-61.
8. Méndez RA, Wunderink W, Hussain SM, et al. Stereotactic body radiation therapy for primary and metastatic liver tumors: A single institution phase i-ii study. *Acta Oncol*. 2006;45:831-837.
9. Velec M, Haddad CR, Craig T, et al. Predictors of liver toxicity following stereotactic body radiation therapy for hepatocellular carcinoma. *Int J Radiat Oncol Biol Phys*. 2017;97:939-946.
10. Barry AS, McPartlin AJ, Lindsay PE, et al. Dosimetric associations with acute liver toxicity in stereotactic body radiation therapy for liver metastases. *Int J Radiat Oncol Biol Phys*. 2016;96:E201-E202.
11. Barry A, McPartlin A, Lindsay P, et al. Dosimetric analysis of liver toxicity after liver metastasis stereotactic body radiation therapy. *Pract Radiat Oncol*. 2017;7:e331-e337.
12. Koay EJ, Owen D, Das P. Radiation-induced liver disease and modern radiotherapy. *Semin Radiat Oncol*. 2018;28:321-331.
13. Schaub SK, Apisarnthanarax S, Price RG, et al. Functional liver imaging and dosimetry to predict hepatotoxicity risk in cirrhotic patients with primary liver cancer. *Int J Radiat Oncol Biol Phys*. 2018;102:1339-1348.
14. Toya R, Saito T, Kai Y, et al. Impact of 99mTc-GSA SPECT image-guided inverse planning on dose−function histogram parameters for stereotactic body radiation therapy planning for patients with hepatocellular carcinoma: A dosimetric comparison study. *Dose-response*. 2019;17:1559325819832149.
15. Fode MM, Petersen JB, Sørensen M, Holt MI, Keiding S, Høyer M. 2-[18F]fluoro-2-deoxy-d-galactose positron emission tomography guided functional treatment planning of stereotactic body radiotherapy of liver tumours. *Phys Imaging Radiat Oncol*. 2017;1:28-33.
16. Ohira S, Kanayama N, Toratani M, et al. Stereotactic body radiation therapy planning for liver tumors using functional images from dual-energy computed tomography. *Radiother Oncol*. 2020;145:56-62.
17. Tsegmed U, Kimura T, Nakashima T, et al. Functional image-guided stereotactic body radiation therapy planning for patients with hepatocellular carcinoma. *Med Dosim*. 2017;42:97-103.
18. Ayuso C, Rimola J, Vilana R, et al. Diagnosis and staging of hepatocellular carcinoma (HCC): Current guidelines. *Eur J Radiol*. 2018;101:72-81.
19. Nilsson H, Nordell A, Vargas R, Douglas L, Jonas E, Blomqvist L. Assessment of hepatic extraction fraction and input relative blood flow using dynamic hepatocyte-specific contrast-enhanced MRI. *J Magn Reson Imaging*. 2009;29:1323-1331.
20. Sourbron S, Sommer WH, Reiser MF, Zech CJ. Combined quantification of liver perfusion and function with dynamic gadoxetic acid −enhanced MR imaging. *Radiology*. 2012;263:874-883.
21. Phonlakrai M, Ramadan S, Simpson J, et al. Determination of hepatic extraction fraction with gadoxetate low-temporal resolution DCE-MRI-based deconvolution analysis: Validation with ALBI score and Child-Pugh class. *J Med Radiat Sci*. 2023;70(suppl 2):48-58.
22. Huh J, Ham SJ, Cho YC, et al. Gadoxetate-enhanced dynamic contrast-enhanced MRI for evaluation of liver function and liver fibrosis in preclinical trials. *BMC Med Imaging*. 2019;19:89.
23. Gjini M, Velten C, Brodin P, et al. Association between liver imaging changes after liver SBRT as estimated by area under the dynamic contrast-enhanced MRI curve and changes in global liver function. *Int J Radiat Oncol Biol Phys*. 2022;114:S50-S51.
24. Noël G, Antoni D. Organs at risk radiation dose constraints. *Cancer Radiothér*. 2022;26:59-75.
25. Klein S, Staring M, Murphy K, Viergever MA, Pluim JP. Elastix: A toolbox for intensity-based medical image registration. *IEEE Trans Med Imaging*. 2009;29:196-205.
26. Brock KK, Mutic S, McNutt TR, Li H, Kessler ML. Use of image registration and fusion algorithms and techniques in radiotherapy: Report of the AAPM radiation therapy committee task group no. 132. *Med Phys*. 2017;44:e43-e76.
27. Jackson WC, Hartman HE, Gharzai LA, et al. The potential for mid-treatment Albumin-Bilirubin (ALBI) score to individualize liver

stereotactic body radiation therapy. *Int J Radiat Oncol Biol Phys*. 2021;111:127-134.
28. Bland JM, Altman DG. Multiple significance tests: The Bonferroni method. *BMJ*. 1995;310:170.
29. Ye L, Liang R, Zhang J, et al. Postoperative albumin-bilirubin grade and albumin-bilirubin change predict the outcomes of hepatocellular carcinoma after hepatectomy. *Ann Transl Med*. 2019;7:367.
30. Ho SY, Liu PH, Hsu CY, et al. Comparison of twelve liver functional reserve models for outcome prediction in patients with hepatocellular carcinoma undergoing surgical resection. *Sci Rep*. 2018;8:4773.
31. Xu W, Li R, Liu F. Novel prognostic nomograms for predicting early and late recurrence of hepatocellular carcinoma after curative hepatectomy. *Cancer Manag Res*. 2020:1693-1712.
32. Shi JY, Sun LY, Quan B, et al. A novel online calculator based on noninvasive markers (ALBI and APRI) for predicting post-hepatectomy liver failure in patients with hepatocellular carcinoma. *Clin Res Hepatol Gastroenterol*. 2021;45:101534.
33. Fagenson AM, Gleeson EM, Pitt HA, Lau KN. Albumin-bilirubin score vs model for end-stage liver disease in predicting post-hepatectomy outcomes. *J Am Coll Surg*. 2020;230:637-645.
34. Kao WY, Su CW, Chiou YY, et al. Hepatocellular carcinoma: nomograms based on the albumin-bilirubin grade to assess the outcomes of radiofrequency ablation. *Radiology*. 2017;285:670-680.
35. Oh IS, Sinn DH, Kang TW, et al. Liver function assessment using albumin−bilirubin grade for patients with very early-stage hepatocellular carcinoma treated with radiofrequency ablation. *Dig Dis Sci*. 2017;62:3235-3242.
36. Lasley FD, Mannina EM, Johnson CS, et al. Treatment variables related to liver toxicity in patients with hepatocellular carcinoma, Child-Pugh class A and B enrolled in a phase 1-2 trial of stereotactic body radiation therapy. *Pract Radiat Oncol*. 2015;5:e443-e449.
37. Dawson LA, Normolle D, Balter JM, McGinn CJ, Lawrence TS. Ten Haken RK. Analysis of radiation-induced liver disease using the Lyman NTCP model. *Int J Radiat Oncol Biol Phys*. 2002;53:810-821.
38. Normolle D, Pan C, Ben-Josef E, Lawrence T. Adaptive trial of personalized radiotherapy for intrahepatic cancer. *Per Med*. 2010;7:197-204.
39. Feng M, Suresh K, Schipper MJ, et al. Individualized adaptive stereotactic body radiotherapy for liver tumors in patients at high risk for liver damage: A phase 2 clinical trial. *JAMA Oncol*. 2018;4:40-47.